HHS Public Access

Author manuscript

J Membr Biol. Author manuscript; available in PMC 2017 August 01.

Published in final edited form as:

J Membr Biol. 2016 August ; 249(4): 539–549. doi:10.1007/s00232-016-9896-z.

Heterogeneous Inhibition in Macroscopic Current Responses of Four Nicotinic Acetylcholine Receptor Subtypes by Cholesterol Enrichment

Carlos A. Báez-Pagán[1,2,3], **Natalie del Hoyo-Rivera**[4], **Orestes Quesada**[3], **José David Otero-Cruz**[1], and **José A. Lasalde-Dominicci**[1,2]

Carlos A. Báez-Pagán: cbaezpagan@gmail.com; José A. Lasalde-Dominicci: jlasalde@gmail.com

[1]Department of Biology, University of Puerto Rico, Río Piedras Campus, PO Box 23360, San Juan, PR 00931, USA

[2]Molecular Sciences Research Center, University of Puerto Rico, San Juan, PR, USA

[3]Department of Physical Sciences, University of Puerto Rico, Río Piedras Campus, PO Box 23323, San Juan, PR 00931, USA

[4]School of Pharmacy, Medical Sciences Campus, University of Puerto Rico, San Juan, PR, USA

Abstract

The nicotinic acetylcholine receptor (nAChR), located in the cell membranes of neurons and muscle cells, mediates the transmission of nerve impulses across cholinergic synapses. In addition, the nAChR is also found in the electric organs of electric rays (e.g., the genus *Torpedo*). Cholesterol, which is a key lipid for maintaining the correct functionality of membrane proteins, has been found to alter the nAChR function. We were thus interested to probe the changes in the functionality of different nAChRs expressed in a model membrane with modified cholesterol to phospholipid ratios (C/P). In this study, we examined the effect of increasing the C/P ratio in *Xenopus laevis* oocytes expressing the neuronal α7, α4β2, muscle-type, and *Torpedo californica* nAChRs in their macroscopic current responses. Using the two-electrode voltage clamp technique, it was found that the neuronal α7 and *Torpedo* nAChRs are significantly more sensitive to small increases in C/P than the muscle-type nAChR. The peak current versus C/P profiles during enrichment display different behaviors; α7 and *Torpedo* nAChRs display a hyperbolic decay with two clear components, whereas muscle-type and α4β2 nAChRs display simple monophasic decays with different slopes. This study clearly illustrates that a physiologically relevant increase in membrane cholesterol concentration produces a remarkable reduction in the macroscopic current responses of the neuronal α7 and *Torpedo* nAChRs functionality, whereas the muscle nAChR appears to be the most resistant to cholesterol inhibition among all four nAChR subtypes. Overall, the present study demonstrates differential profiles for cholesterol inhibition among the different types of nAChR to physiological cholesterol increments in the plasmatic membrane. This is the first study to report a cross-correlation analysis of cholesterol sensitivity among different nAChR subtypes in a model membrane.

Correspondence to: Carlos A. Báez-Pagán, `cbaezpagan@gmail.com`; José A. Lasalde-Dominicci, `jlasalde@gmail.com`.

Carlos A. Báez-Pagán and Natalie del Hoyo-Rivera have contributed equally to this work.

Keywords

Cholesterol; Nicotinic acetylcholine receptor; Ion channels; Regulation; Membrane proteins

Introduction

The nicotinic acetylcholine receptor (nAChR) is a membrane-embedded protein responsible for neurotransmission across different types of synapses. The nAChR belongs to the family of ligand gated ion channels (LGIC), which includes the glycine receptors, the γ-aminobutyric acid type A receptors ($GABA_A$), and the serotonin 5-HT_3 receptors (Cockcroft et al. 1990; Corringer et al. 2000; Karlin 2002; Le Novère et al. 2002). These ion channel receptors have a pentameric assembly of five subunits arranged about a central cation-selective pore (Cockcroft et al. 1990; Corringer et al. 2000; Karlin 2002; Le Novère et al. 2002). The main role of the nAChRs is neurotransmission across different types of synapses where it mediates neuronal communications and muscle contractions. The nAChRs are located in the plasma membranes of neurons, immune cells, muscle cells, and electrocytes—cells from the electric organ found in electric rays such as those from the genus *Torpedo*—(Galzi et al. 1991). The neuronal nAChRs are commonly found in the basal fore-brain, hippocampus, and temporal cortex. These brain locations are considered to be involved in learning and memory. The neuronal receptors comprise one or two types of subunits, namely α and β, with various stoichiometries. In addition, the α subunit forms homopentameric receptors such as the neuronal α7 nAChR (Cooper et al. 1991; Paterson and Nordberg 2000; Itier and Bertrand 2001). In muscle cells, however, the nAChR comprises α, β, ε, and δ subunits arranged in a 2:1:1:1 stoichiometric ratio, whereas the *Torpedo californica* nAChR comprises α, β, γ, and δ subunits arranged too in a 2:1:1:1 stoichiometric ratio (Galzi et al. 1991).

As with other membrane-embedded proteins, cholesterol modulates the activity of the nAChR (Dalziel et al. 1980; Fong and McNamee 1986; Burger et al. 2000). The rigid polycyclic structure of cholesterol straightens the acyl chains of phospholipids leading to a reduction in membrane fluidity (Demel et al. 1972; Gally et al. 1976; Yeagle 1985; Radhakrishnan and McConnell 1999; McConnell and Radhakrishnan 2003). The effect of cholesterol in membrane fluidity has been hypothesized to be involved in the regulation of the nAChR function (Burger et al. 2000; Barrantes 2004); however, other alternative hypotheses have been put forward including specific binding sites for cholesterol within the nAChR lipid-protein interface (Fong and McNamee 1986; Leibel et al. 1987; Middlemas and Raftery 1987; Jones and McNamee 1988; Addona et al. 1998). Regardless of its specific mode of action, the effects of cholesterol in the nAChR function appear to be related to the concentration of cholesterol in the plasmalemma (Santiago et al. 2001).

The lipid composition of cell membranes has been shown to modulate the functionality of membrane proteins (Lee 2003; Jensen and Mouritsen 2004). As aforementioned, the cholesterol concentration in cell membranes is of fundamental importance in modulating the functionality of many membrane proteins (Burger et al. 2000; Barrantes 2002; Abi-Char et al. 2007). The cholesterol concentration in cell membranes is highly regulated and different

cell types normally have their characteristic plasmalemma cholesterol concentration (Schiebler and Hucho 1978; Gonzalez-Ros et al. 1982). Along these lines, the functionality of membrane proteins should change when expressed in different cell types. In the present study, we examined the functionality of different nAChR subtypes expressed in *Xenopus laevis* oocytes (Sumikawa et al. 1981) in which the cholesterol to phospholipids ratios (C/P) were increased using cholesterol-enriched liposomes. We assessed the macroscopic current response elicited by α7, α4β2, muscle-type, and *Torpedo californica* nAChRs expressed in *Xenopus* oocytes, upon increasing the oocytes C/P by 13.0, 24.4 and 38.9 %. The macroscopic response of all four nAChR subtypes was significantly reduced as the C/P ratio increased; however, two of the nAChR subtypes, namely *Torpedo* californica and α7 nAChRs, displayed stepwise reductions in macroscopic current. In contrast, the reduction in macroscopic response of the muscle-type nAChR and neuronal α4β2, display a different profile. The present data demonstrate that a 13.0 % increase in the oocytes C/P had little to moderate effects in the muscle-type and α4β2, whereas the same increase in C/P resulted in substantial reductions in macroscopic functional response in the α7 and *Torpedo californica* nAChRs. The relatively less susceptibility to membrane cholesterol concentration displayed by the muscle-type and α4β2 nAChRs could be indicative of a mechanism by which these nAChR subtypes cope with increasing cholesterol concentrations that may result from aging (Cohen and Zubenko 1985; Krainev et al. 1995; Wood et al. 2002).

Materials and Methods

Cholesterol Enrichment of *Xenopus laevis* Oocytes

The membrane cholesterol concentration of *Xenopus laevis* oocytes was increased by means of 15, 30, and 45 min incubations in 30 μL of cholesterol-enriched liposomes prepared using the cholesterol removal technique as described previously (Santiago et al. 2001). In brief, a 1:1 molar ratio solution containing cholesterol and 1,2-Di-oleoyl-*sn*-Glycero-3-Phosphocholine (DOPC) was prepared in chloroform and dried under a stream of nitrogen. 1 mL of a sodium cholate solution prepared in NaCl 0.9 % was added to the dried lipids to achieve a 1:1:2 cholesterol/ DOPC/cholate molar ratio and mixed thoroughly. Detergent removal was subsequently accomplished at constant temperature using the Mini-Lipoprep-Dialyzer and a DIACHEMA membrane (mw.-cutoff 10,000).

Determination of Membrane Cholesterol in *Xenopus laevis* Oocytes

Membrane Isolation—Six batches of oocytes (30 oocytes/batch) were used for each analysis. Three batches of oocytes were incubated in cholesterol-enriched liposomes and three in MOR2 buffer (115 mM NaCl, 2.5 mM KCl, 5 mM $MgCl_2$, 1 mM Na_2 HPO_4, 5 mM HEPES, 0.2 mM $CaCl_2$, pH 7.4) (control experiment) for 15, 30, or 45 min and then washed. Membrane isolation was performed as described by Ohlsson et al. (Ohlsson et al. 1981) with minor modifications. Briefly, two-phase sucrose gradients were prepared with 1.5 and 0.3 M sucrose buffers (20 mM Tris HCl, 50 mM KCl, 10 mM $MgCl_2$, 1 mM EGTA, pH 7.6,) at a 1:2 ratio in 1.5-mL microtubes (30 oocytes/microtube). The oocytes from each batch were manually disrupted with forceps, layered at the upper phase of the separation medium, and centrifuged for 20 min at 12,000 ×*g* (4 °C). The interface between the phases containing the membranes was removed, washed (5.0 mM HEPES, 160 mM NaCl, pH 7.4), and

centrifuged for 10 min at 3000×*g* (4 °C). The pellet was resuspended in 200 μL of MOR2 buffer and sonicated.

Quantization of Membrane Cholesterol/Phospholipid (C/P) Ratio—Total lipids from the plasmatic membrane of oocytes was extracted overnight at 4 °C under a nitrogen atmosphere with chloroform:methanol (2:1, v:v) containing butylated hydroxytoluene (BHT), 2×10^{-5} M. Quantization of the membrane phospholipids was achieved by subjecting the extracted lipid from the *Xenopus laevis* oocyte plasma membrane to an acid hydrolysis. After 3.5 h of reflux with methanol/HCl, all the fatty acids were converted to fatty acid methyl esters (FAME). This nonaqueous acid system is the most suitable for the hydrolysis of the fatty acyl amide bond of sphingolipids. Under these experimental conditions almost all acyl chains in the phospholipids are converted to their respective FAME. Quantization of the individual components of the fatty acid mixture was accomplished by adding an internal standard (IS) ($20:1^{\Delta 11}$) of known concentration, which is absent in the lipids from the *Xenopus laevis* oocyte's plasmalemma. The FAME, the free fatty acids, and the IS were extracted with petroleum ether and dried under nitrogen. The extract was dissolved in 10 % methanol/diethyl ether and the free fatty acids were methylated using 0.5 mL of diazomethane. After 20 min, the reaction mixture was extracted with petroleum ether. The FAME were separated from other lipids on rhodamine 6G stained silica gel G plates with petroleum ether/diethyl ether (98:2, v/v) as the solvent system. The spots corresponding to the FAME and cholesterol were extracted with petroleum ether:ethyl ether (2:3, v/v). Then the FAME were analyzed with a Hewlett-Packard 5890 gas chromatographer using a glass column packed with GP 10 % SP 100/120 Cromosorb (155–250 °C). Peak identification was carried out isothermally by comparison with known standard mixtures and by graphical correlation to equivalent chain length values. Since each phospholipid produces two fatty acids under the total hydrolysis conditions stated above, the total of phospholipids from the samples were determined by dividing the total FAME by two. Contamination by trace amounts of fatty acids, particularly palmitic (16:0), stearic (18:0), and oleic (18:1), which were found in all the solvents tested, was eliminated in each experiment by the appropriate use of control samples to which lipids were not added. The cholesterol isolated from the rhodamine 6G stained silica gel G plates was assayed using the Wako cholesterol E Kit (Wako Chemicals, Richmond VA) according to the manufacturer's indications. In brief, cholesterol esters in the sample were hydrolyzed in a reaction catalyzed by cholesterol ester hydrolase and then oxidized by cholesterol oxidase, which generates hydrogen peroxide. The formed hydrogen peroxide then participates in a quantitative oxidative condensation reaction between 3,5-dimethoxy-N-ethyl-N-(2-hydroxy-3-sulfopropyl)-aniline sodium salt (DAOS) and 4-aminoantipyrine in the presence of peroxidase to produce a blue pigment. The cholesterol in the sample was determined by measuring the absorbance of the blue color at 600 nm. The total cholesterol concentration corresponding to the absorbance of the sample was read from a calibration curve prepared in advanced and divided by the determined total of phospholipids to calculate the C/P.

Imaging Experiments—*Xenopus laevis* oocytes were incubated for 15, 30, or 45 min in 30 μL of DOPC liposomes enriched in the cholesterol fluorescent analog [(22-(N-(7-nitrobenz-2-oxa-1,3-diazol-4-yl)amino-22,23-bisnor-5-cholen-3-ol)] prepared as described

previously (Santiago et al. 2001). Upon incubation, the oocytes were washed three times in MOR2 buffer. The incorporation of the fluorescent cholesterol analog into the plasmalemma of *Xenopus laevis* oocytes was monitored by exciting at a wavelength of 488 nm using an Argon/2 laser and its emission acquired using a BP 500–550 on a Zeiss LSM 510 Confocal Microscope. The magnification used was 10X. Images were acquired as single optical slices. Appropriate control experiments were performed to access the oocytes autofluorescence under the same imaging parameters.

Expression of the Different nAChR Subtypes in Xenopus laevis Oocytes— RNA transcripts were synthesized in vitro as described previously (Lee et al. 1994). The RNA transcripts of the *Torpedo californica*, muscle (*Mus musculus*), α4β2 (*Rattus norvegicus*), or α7 (human) nAChR subunits were injected into *Xenopus laevis* oocytes in the V or VI developmental stage. The *Torpedo californica* α, β, γ, and δ subunits and muscle-type α, β, ε, and δ subunits were microinjected in a 2:1:1:1 ratio, and the α4β2 was microinjected in a 2:3 ratio. Upon microinjection, the oocytes were incubated at 19 °C for 72–96 h in a medium containing 50 % Leibovitz's L-15 media (GIBCO, Gaithersburg, MD), 0.4 mg/mL bovine serum albumin and antibiotic-antimycotic agents added according to manufacturer's directions prior to the scheduled experiments. All animal procedures were done in accordance with the guidelines and with the approval of the University of Puerto Rico Institutional Animal Care and Utilization Committee (Protocol No. ATP001-07-12-2013). The liquid medium was changed regularly.

Voltage Clamp Recordings

Determination of Reduction in Macroscopic Response

Two-electrode voltage clamp macroscopic currents evoked by 100 μM acetylcholine (ACh) were recorded using a Gene Clamp 500B amplifier (Axon Instruments, Foster City, CA) before and after cholesterol enrichment. Electrodes were filled with 3 M KCl and had a resistance of less than 2 MΩ. Impaled oocytes in the recording chamber were automatically perfused using a Perfusion Valve Controller VC-8 (Warner Instruments, Inc., Hamden, CT.) at a rate of approximately 0.5 mL/s with MOR2 buffer. Oocytes were held at a membrane potential of −70 mV. Membrane currents were filtered at 0.1 kHz and digitized at 1 kHz using a Digidata 1322A interface (Axon Instruments, Foster City, CA) and acquired using the Clampex 9.2, pCLAMP 9.2 software package (Axon Instruments, Foster City, CA).

Results

Cholesterol Enrichment of Xenopus laevis Oocytes Plasmalemma

The *Xenopus laevis* oocytes cholesterol/phospholipid molar ratio (C/P) was determined upon 15, 30, or 45 min incubations in cholesterol-rich liposomes. After these incubations, the oocytes' plasmalemma was isolated and the C/P was determined as described in the "Materials and Methods" section. As displayed in Fig. 1a, the C/P of oocytes incubated in MOR2 buffer (control experiments) was determined to be 0.316 ± 0.009 (mean ± SEM). Incubation of oocytes in cholesterol-rich DOPC liposomes for 15 min significantly increased the oocytes plasmalemma C/P to 0.357 ± 0.005 (One-way ANOVA with Dunnett's post-test;

P value <0.01; *n* = 4), which corresponds to a 13.0 % increase in C/P. Incubation of oocytes in liposomes for 30 min increased the C/P to 0.393 ± 0.003 (One-way ANOVA with Dunnett's post-test; *P* value <0.001; *n* = 4) corresponding to a 24.4 % increase in C/P, and 45 min incubations resulted in a 38.9 % increase, corresponding to a C/P of 0.439 ± 0.008 (One-way ANOVA with Dunnett's post-test; *P* value <0.01; *n* = 4). However, these incubations did not result in statistically significant changes in the fatty acid concentrations (Fig. 1b) (Two-way ANOVA with Bonferroni's post-test, *P* > 0.05).

To provide further evidence of the incorporation of cholesterol to the *Xenopus laevis* oocytes plasmalemma through incubations in cholesterol-rich liposomes, an alternate methodology was used. In these experiments, DOPC liposomes were enriched with the fluorescent cholesterol analog [(22-(N-(7-nitrobenz-2-oxa-1,3-diazol-4-yl)amino-22,23-bisnor-5-cholen-3-ol)] rather than with cholesterol, and the incorporation of this fluorescent molecule into the *Xenopus laevis* oocytes plasma membrane was monitored by confocal microscopy. Figure 2 summarizes the results of these experiments. Incubation of oocytes for 15 min in liposomes enriched with the cholesterol fluorescent analog resulted in a (112 ± 21) % (mean ± SEM) increase (One-way ANOVA with Dunnett's post-test; *P* value <0.05; *n* = 5) in fluorescence intensity when compared to the fluorescence of oocytes not incubated in liposomes (autofluorescence control). Incubation of oocytes for 30 and 45 min in liposomes produced increases in fluorescence intensity of (196 ± 35) % (Oneway ANOVA with Dunnett's post-test; *P* value <0.01; *n* = 5) and (419 ± 29) % (One-way ANOVA with Dunnett's post-test; *P* value <0.01; *n* = 5), respectively.

Cholesterol Enrichment Effects in Macroscopic Response

We were interested in determining the effects of membrane cholesterol enrichment in the functionality of four different nAChR subtypes, namely *Torpedo californica*, muscle, α4β2, and α7 nAChRs, when expressed in *Xenopus laevis* oocytes. To achieve this, we incubated oocytes expressing the nicotinic receptor under study in DOPC liposomes enriched with cholesterol for 15, 30, and 45 min, which increased the oocytes C/P by 13.0, 24.4, and 38.9 %, respectively (Fig. 1). The peak currents elicited by 100 μM ACh in oocytes expressing the nAChR subtypes studied were determined prior to the first incubation and after every subsequent incubation. Figures 3 and 4 present the results of these experiments for the muscle and *Torpedo californica* nAChRs (Fig. 3), and for the neuronal nAChRs α7 and α4β2 (Fig. 4). A 13 % increase in the C/P of oocytes (15 min incubation in cholesterol-rich liposomes) resulted in statistically significant differences in the corresponding reductions in macroscopic currents with a (28 ± 4) % (mean ± SEM) decrease in peak current in oocytes expressing the *Torpedo californica* nAChR compared to a (8 ± 5) % decrease in the muscle nicotinic receptor, (35 ± 5) % in the α7, and (16 ± 3) % in the α4β2 nicotinic receptor. The differences in the extent of the inhibition in function were found to be statistically significant when the muscle nAChR was compared to the *Torpedo californica* nAChR (*P* value = 0.0095), when the muscle nAChR was compared to the α7 nAChR (*P* value = 0.0035), when *Torpedo* was compared to α4β2 (*P* value = 0.0126), and when the α7 was compared to the α4β2 (*P* value = 0.0006) (Table 1).

When the oocytes were incubated in cholesterol-rich DOPC liposomes for 30 min, the *Torpedo californica*, muscle, α7, and α4β2 nAChRs displayed decreases in macroscopic currents corresponding to (26 ± 4), (29 ± 7), (35 ± 6), and (22 ± 5) %, respectively, and when the oocytes were incubated in cholesterol-rich DOPC liposomes for 45 min, the *Torpedo californica* nAChR, muscle, α7, and α4β2 nAChRs displayed decreases in macroscopic currents corresponding to (38 ± 9), (46 ± 5), (52 ± 8), and (34 ± 6) %, respectively. However, the differences in the extent of the decrease in macroscopic currents between the four nicotinic receptor subtypes upon 30 and 45 min incubations did not reach statistical significance. Table 1 summarizes the results of these experiments.

Discussion

Cholesterol Modulates nAChR Function

The nAChR-cholesterol interactions are known to regulate the function and number of nAChRs; however, the underlying mechanisms are poorly understood. Previous studies have postulated at least two possible mechanisms to explain the effects of cholesterol on the modulation of nAChR functionality. The first hypothesis proposes that the action of cholesterol on the nAChR might be associated with the bulk-lipid bilayer fluidity (Fong and McNamee 1986; Sunshine and McNamee 1992; Baenziger et al. 2000). The second hypothesis suggests that cholesterol may act as an “allosteric effector” at some nonannular or interstitial binding sites located within the protein that are distinct from the lipid-protein interface (Jones and McNamee 1988; Narayanaswami and McNamee 1993; Fernandez-Ballester et al. 1994; Antollini and Barrantes 1998). The binding sites for cholesterol lipid-protein at the interface of the *Torpedo* AChR were mapped using a photoreactive analog of cholesterol (125I-azido-cholesterol) (Corbin et al. 1998). In the aforementioned study, cholesterol-binding sites were found exclusively in the αM4 and αM1 and γM4 transmembrane segments. Cholesterol-binding sites were also found exclusively in the M4, M3, and Ml of each subunit; thus, the cholesterol-binding domain fully overlaps the lipid interface of the *Torpedo* nAChR (Hamouda et al. 2006). Molecular dynamic simulations studies predicted sites at the protein-lipid interface, consistent with functional data, but also deeply buried sites (Brannigan et al. 2008). A question remains as to the nature of the molecular mechanisms that could be responsible for the effects of cholesterol in modulating nAChR function. The cholesterol inhibition of nAChR functionality is a central aspect of this study. There is a limited amount of studies that have examined the effects of cholesterol enrichment on nAChR function in cell membrane models (Lechleiter et al. 1986; Lasalde et al. 1995; Antollini and Barrantes 1998; Santiago et al. 2001; Barrantes 2002, 2004).

We expressed four different subtypes of nicotinic receptors, namely the *Torpedo californica*, muscle, and neuronal α7 and α4β2 nAChRs in a membrane model and assessed the changes in the nicotinic receptor function upon cholesterol enrichment of the plasmalemma (Sumikawa et al. 1981). By incubating oocytes in cholesterol-rich DOPC liposomes for 15, 30, and 45 min, we successfully increased the plasmalemma C/P by 13.0, 24.4, and 38.9 %, respectively (Fig. 1), an observation consistent with the increase in fluorescence in *Xenopus laevis* oocytes incubated in DOPC liposomes enriched with the cholesterol fluorescent analog [(22-(N-(7-nitrobenz-2-oxa-1,3-diazol-4-yl)amino-22,23-bisnor-5-cholen-3-ol)] (Fig.

2). Upon cholesterol enrichment, the macroscopic response in each nicotinic receptor subtype was assessed through voltage clamp.

Cholesterol Enrichment Leads to Dissimilar Inhibition of nAChRs Function

Cholesterol enrichment resulted in dissimilar decreases in macroscopic response in all four nicotinic receptor subtypes under study (Fig. 5). This inhibition in response did not follow a linear tendency in two of the nicotinic receptors studied (*Torpedo californica* and α7 nAChRs); the first 15 min incubations resulted in a remarkable decrease in macroscopic response. However, the next 15 min incubations (30 min total) did not result in further decreases in macroscopic response, a behavior reminiscent to the formation of a plateau. Nevertheless, the following 15 min incubations (45 min total) resulted in additional inhibition of response. In essence, the profiles of the inhibition in response in these two nAChR subtypes were characterized by two sharp reductions in macroscopic current separated by a short plateau, suggesting the existence of two different underlying mechanisms as cause for the observed decrease in macroscopic current (Figs. 3, 4). While the *Torpedo californica* and the α7 nAChR had similar inhibition profiles, the muscle nAChR, and to a lesser extent the α4β4, differed in the inhibitory profiles because the first 15 min incubations did not result in substantial reductions in macroscopic response. Interestingly, the only homomeric receptor studied, the α7 nAChR, showed the highest cholesterol-induced reduction in macroscopic current. The observation that the homomeric receptor is also the most affected by the cholesterol enrichment leads us to hypothesize that specific amino acids, or a motif within the α7 subunit, and shared by some subunits, provide an additive effect that affects mostly the receptor comprising five copies of the α7 subunit.

Cholesterol Concentration in the Plasmalemma and the Stability of the Open Channel Conformation

The aforementioned results lead to a fundamental question: Why is the muscle nAChR function more resistant to small increases in membrane C/P than its homologous *Torpedo californica* nAChR? The *Torpedo californica* nAChR possesses a high degree of homology with the muscle-type nAChR (Guzmán et al. 2006; Kalamida et al. 2007). However, in spite of the high degree of homology between these two subtypes of nicotinic receptors, there are differences in their ion channel kinetics. Indeed, both of these subtypes of receptors have been thoroughly characterized by various groups. For instance, the mean open time of the *Torpedo californica* nAChR at low ACh concentrations (1.0 μM) has been estimated to be 0.2–0.3 ms compared to 3.75 ms in the muscle nicotinic receptor (Lee et al. 1994; Tamamizu et al. 1999, 2000). Therefore, upon activation of the *Torpedo californica* nAChR by ACh, this subtype spends considerably less time in the open state when compared to the muscle nAChR, which suggests that the open conformation of the muscle nicotinic receptor is more stable than the open conformation of the *Torpedo californica*. Interestingly, the trend in the open state stability coincides with the trend observed in the inhibition in function observed by 13 % increases in membrane cholesterol concentration. This observation may be interpreted as to suggest that the inhibition in the function of the muscle and *Torpedo* nicotinic receptors upon cholesterol enrichment may be related to a concomitant decrease in the stability of the open conformation, which would, presumably, have more pronounced effects in the more labile open state of the *Torpedo californica*.

Cholesterol Inhibition of nAChR and Membrane Rafts

Cholesterol is a key component of the membrane micro-domains known as membrane rafts, which have been defined as small, heterogeneous, highly dynamic, sterol-and sphingolipid-enriched domains that compartmentalize cellular processes and that can sometimes be stabilized to form larger platforms through protein-protein and protein-lipid interactions (Pike 2006). Indeed, cholesterol depletion disrupts membrane rafts, a process which has been suggested to lead to the redistribution of the proteins located therein to the bulk membrane (Oshikawa et al. 2003; Ikonen et al. 2004; Barbuti et al. 2004). Along the same line, several types of nAChRs have already been found in membrane rafts including the α7 nAChR (Brusés et al. 2001; Marchand et al. 2002; Oshikawa et al. 2003; Zhu et al. 2006). Thus, a potential model to explain the current results may include the aggregation of nicotinic receptors in cholesterol-rich domains as a consequence of the increase in membrane cholesterol concentration. Cholesterol-rich domains may constitute a nonactivatable pool of receptors, which suggests that differences in the affinities between the four nicotinic receptor subtypes studied and cholesterol-rich domains could explain the differences in the inhibition profiles summarized in Fig. 5. Indeed, we previously showed that the cholesterol-sensitive αC418W nAChR mutation present in caveolin-1-positive domains appear to be in a *nonactivatable* state (Báez-Pagán et al. 2008), and that the expression of the αC418W nAChR in transgenic mice leads to the accumulation of caveolin-1 in endplates (Grajales-Reyes et al. 2013). An implicit assumption of this potential model is that the muscle nAChR would display less affinity towards cholesterol-rich domains and therefore remain functional at membrane cholesterol concentrations at which the macroscopic currents of the *Torpedo californica* and the α7 nicotinic receptors are remarkably reduced.

Cholesterol and Neuronal nAChR Function: Potential Implication in Cognitive Disruption

It has been documented that learning deficits in Alzheimer's disease can be presented even before any observable cell loss, suggesting that the initial disruption of cognitive function in this disease is not due to cell death, but rather due to the disruption of neuronal nAChRs and synaptic transmission (O'Neill et al. 2002). Along these lines, epidemiological evidence has suggested that high cholesterol is a risk factor for Alzheimer's disease (Roher et al. 1999). The physiological effects of cholesterol on the neuronal nAChR function could have paramount implications if we consider that a 13 % increment in C/P can reduce α7 currents by 35 %, as observed in the present study. Understanding the regulation of cholesterol on neuronal nAChRs subtypes is of tremendous importance; however, this aspect of the nAChR has remained obscure. To our best understanding, a very small number of research laboratories groups have focused on this fundamental aspect of the nAChR function. The present study provides new insights into the sensitivity of α7-nAChR to the cholesterol concentration in the plasma membrane. It is noteworthy that both α7 nAChR and dysregulation of cholesterol metabolism have been implicated in the development of Alzheimer's disease (AD). Along these lines, previous studies proposed that development of AD is characterized by both cholesterol dysregulation and a degeneration of cholinergic neurons (Barrantes et al. 2010). Understanding the structural and functional basis for the remarkable cholesterol-induced inhibition of the neuronal α7 nAChR is of biological

importance, especially in the context of its potential implications in the cognitive deficits observed during neurodegenerative diseases.

Conclusion

The present study has systematically assessed the consequences of increasingly higher membrane cholesterol concentrations in the function of the nAChR. In doing so, it has revealed the relatively high tolerance of the muscle nicotinic receptor to the lowest increase in membrane C/P studied (13.0 %). Another interesting observation that results from this study is that neuronal receptors do not respond to 13.0 % increases in C/P to similar extents. Indeed, the reduction in α7 macroscopic current is similar to the reduction observed in the *Torpedo* nAChR, and the reduction in α4β2 macroscopic current is similar to the muscle-type nAChR. These results reveal that cholesterol sensitivity cannot be predicted on the basis of whether the receptor is neuronal or not, and suggest that specific amino acids or motif could determine cholesterol sensitivity. The specific structural basis for the cholesterol sensitivity of nicotinic receptors remains to be identified. Furthermore, the present study also uncovers that at high enough cholesterol concentrations (beyond a 24.4 % increase) all four nicotinic receptors studied display significant inhibition of the macroscopic response. While the inhibition profiles displayed upon large increases in cholesterol concentration provide useful and interesting data, relatively small increases in cholesterol concentrations likely reflect physiologically relevant scenarios. For instance, cholesterol concentrations have been shown to increase with age (Cohen and Zubenko 1985; Krainev et al. 1995; Wood et al. 2002). These findings raise the hypothesis that the muscle-type nAChR may have evolved mechanisms to cope with the increase in cholesterol concentration that accompanies aging. In contrast, the neuronal α7 nAChR seems to be highly sensitive to potential physiological increases of cholesterol.

Acknowledgments

This research was supported by the National Institutes of Health NIGMS grants 1R01GM098343 (JALD) and 1P20GM103642 (J.R. and JALD). The content is solely the responsibility of the authors and does not necessarily represent the official views of the National Institutes of Health. Natalie del Hoyo-Rivera was supported by the UPR-RP MARC Program (Grant Number: 5T34GM07821) (OQ) and by the NIH-MBRS Research Initiative for Scientific Enhancement Grant R25GM61151 (OQ).

Abbreviations

nAChR	Nicotinic acetylcholine receptor
WT	Wild type
ACh	Acetylcholine
α-BTX	α-Bungarotoxin

References

Abi-Char J, Maguy A, Coulombe A, et al. Membrane cholesterol modulates Kv1.5 potassium channel distribution and function in rat cardiomyocytes. J Physiol. 2007; 582:1205–1217. [PubMed: 17525113]

Addona GH, Sandermann H, Kloczewiak MA, et al. Where does cholesterol act during activation of the nicotinic acetyl-choline receptor? Biochim Biophys Acta. 1998; 1370:299–309. [PubMed: 9545586]

Antollini SS, Barrantes FJ. Disclosure of discrete sites for phospholipid and sterols at the protein-lipid interface in native acetylcholine receptor-rich membrane. Biochemistry (Mosc). 1998; 37:16653–16662.

Baenziger JE, Morris ML, Darsaut TE, Ryan SE. Effect of membrane lipid composition on the conformational equilibria of the nicotinic acetylcholine receptor. J Biol Chem. 2000; 275:777–784. [PubMed: 10625607]

Báez-Pagán CA, Martínez-Ortiz Y, Otero-Cruz JD, et al. Potential role of caveolin-1-positive domains in the regulation of the acetylcholine receptor's activatable pool: implications in the pathogenesis of a novel congenital myasthenic syndrome. Channels Austin Tex. 2008; 2:180–190.

Barbuti A, Gravante B, Riolfo M, et al. Localization of pacemaker channels in lipid rafts regulates channel kinetics. Circ Res. 2004; 94:1325–1331. [PubMed: 15073040]

Barrantes FJ. Lipid matters: nicotinic acetylcholine receptor-lipid interactions (Review). Mol Membr Biol. 2002; 19:277–284. [PubMed: 12512774]

Barrantes FJ. Structural basis for lipid modulation of nicotinic acetylcholine receptor function. Brain Res Brain Res Rev. 2004; 47:71–95. [PubMed: 15572164]

Barrantes FJ, Borroni V, Vallés S. Neuronal nicotinic acetylcholine receptor-cholesterol crosstalk in Alzheimer's disease. FEBS Lett. 2010; 584:1856–1863. [PubMed: 19914249]

Brannigan G, Hénin J, Law R, et al. Embedded cholesterol in the nicotinic acetylcholine receptor. Proc Natl Acad Sci USA. 2008; 105:14418–14423. [PubMed: 18768796]

Brusés JL, Chauvet N, Rutishauser U. Membrane lipid rafts are necessary for the maintenance of the (alpha)7 nicotinic acetylcholine receptor in somatic spines of ciliary neurons. J Neurosci Off J Soc Neurosci. 2001; 21:504–512.

Burger K, Gimpl G, Fahrenholz F. Regulation of receptor function by cholesterol. Cell Mol Life Sci CMLS. 2000; 57:1577–1592. [PubMed: 11092453]

Cockcroft VB, Osguthorpe DJ, Barnard EA, et al. Ligand-gated ion channels. Homology and diversity. Mol Neurobiol. 1990; 4:129–169. [PubMed: 1725701]

Cohen BM, Zubenko GS. Aging and the biophysical properties of cell membranes. Life Sci. 1985; 37:1403–1409. [PubMed: 4046740]

Cooper E, Couturier S, Ballivet M. Pentameric structure and subunit stoichiometry of a neuronal nicotinic acetylcholine receptor. Nature. 1991; 350:235–238. [PubMed: 2005979]

Corbin J, Wang HH, Blanton MP. Identifying the cholesterol binding domain in the nicotinic acetylcholine receptor with [125I]azido-cholesterol. Biochim Biophys Acta. 1998; 1414:65–74. [PubMed: 9804895]

Corringer PJ, Le Novère N, Changeux JP. Nicotinic receptors at the amino acid level. Annu Rev Pharmacol Toxicol. 2000; 40:431–458. [PubMed: 10836143]

Dalziel AW, Rollins ES, McNamee MG. The effect of cholesterol on agonist-induced flux in reconstituted acetylcholine receptor vesicles. FEBS Lett. 1980; 122:193–196. [PubMed: 7202709]

Demel RA, Bruckdorfer KR, van Deenen LL. The effect of sterol structure on the permeability of lipomes to glucose, glycerol and Rb + Biochim Biophys Acta. 1972; 255:321–330. [PubMed: 5011000]

Fernandez-Ballester G, Castresana J, Fernandez AM, et al. Role of cholesterol as a structural and functional effector of the nicotinic acetylcholine receptor. Biochem Soc Trans. 1994; 22:776–780. [PubMed: 7821683]

Fong TM, McNamee MG. Correlation between acetylcholine receptor function and structural properties of membranes. Biochem (Mosc). 1986; 25:830–840.

Gally HU, Seelig A, Seelig J. Cholesterol-induced rod-like motion of fatty acyl chains in lipid bilayers a deuterium magnetic resonance study. Hoppe-Seylers Z Für Physiol Chem. 1976; 357:1447–1450.

Galzi JL, Revah F, Bessis A, Changeux JP. Functional architecture of the nicotinic acetylcholine receptor: from electric organ to brain. Annu Rev Pharmacol Toxicol. 1991; 31:37–72. [PubMed: 2064379]

Gonzalez-Ros JM, Llanillo M, Paraschos A, Martinez-Carrion M. Lipid environment of acetylcholine receptor from Torpedo californica. Biochem (Mosc). 1982; 21:3467–3474.

Grajales-Reyes GE, Báez-Pagán CA, Zhu H, et al. Transgenic mouse model reveals an unsuspected role of the acetylcholine receptor in statin-induced neuromuscular adverse drug reactions. Pharmacogenomics J. 2013; 13:362–368. [PubMed: 22688219]

Guzmán GR, Ortiz-Acevedo A, Ricardo A, et al. The polarity of lipid-exposed residues contributes to the functional differences between Torpedo and muscle-type nicotinic receptors. J Membr Biol. 2006; 214:131–138. [PubMed: 17530159]

Hamouda AK, Sanghvi M, Sauls D, et al. Assessing the lipid requirements of the Torpedo californica nicotinic acetylcholine receptor. Biochem (Mosc). 2006; 45:4327–4337.

Ikonen E, Heino S, Lusa S. Caveolins and membrane cholesterol. Biochem Soc Trans. 2004; 32:121–123. [PubMed: 14748728]

Itier V, Bertrand D. Neuronal nicotinic receptors: from protein structure to function. FEBS Lett. 2001; 504:118–125. [PubMed: 11532443]

Jensen MØ, Mouritsen OG. Lipids do influence protein function-the hydrophobic matching hypothesis revisited. Bio-chim Biophys Acta. 2004; 1666:205–226.

Jones OT, McNamee MG. Annular and nonannular binding sites for cholesterol associated with the nicotinic acetylcholine receptor. Biochem (Mosc). 1988; 27:2364–2374.

Kalamida D, Poulas K, Avramopoulou V, et al. Muscle and neuronal nicotinic acetylcholine receptors. Structure, function and pathogenicity. FEBS J. 2007; 274:3799–3845. [PubMed: 17651090]

Karlin A. Emerging structure of the nicotinic acetylcholine receptors. Nat Rev Neurosci. 2002; 3:102–114. [PubMed: 11836518]

Krainev AG, Ferrington DA, Williams TD, et al. Adaptive changes in lipid composition of skeletal sarcoplasmic reticulum membranes associated with aging. Biochim Biophys Acta. 1995; 1235:406–418. [PubMed: 7756351]

Lasalde JA, Colom A, Resto E, Zuazaga C. Heterogeneous distribution of acetylcholine receptors in chick myocytes induced by cholesterol enrichment. Biochim Biophys Acta. 1995; 1235:361–368. [PubMed: 7756346]

Le Novère N, Corringer P-J, Changeux J-P. The diversity of subunit composition in nAChRs: evolutionary origins, physiologic and pharmacologic consequences. J Neurobiol. 2002; 53:447–456. [PubMed: 12436412]

Lechleiter J, Wells M, Gruener R. Halothane-induced changes in acetylcholine receptor channel kinetics are attenuated by cholesterol. Biochim Biophys Acta. 1986; 856:640–645. [PubMed: 2421772]

Lee AG. Lipid-protein interactions in biological membranes: a structural perspective. Biochim Biophys Acta. 2003; 1612:1–40. [PubMed: 12729927]

Lee YH, Li L, Lasalde J, et al. Mutations in the M4 domain of Torpedo californica acetylcholine receptor dramatically alter ion channel function. Biophys J. 1994; 66:646–653. [PubMed: 7516721]

Leibel WS, Firestone LL, Legler DC, et al. Two pools of cholesterol in acetylcholine receptor-rich membranes from Torpedo. Biochim Biophys Acta. 1987; 897:249–260. [PubMed: 2434127]

Marchand S, Devillers-Thiéry A, Pons S, et al. Rapsyn escorts the nicotinic acetylcholine receptor along the exocytic pathway via association with lipid rafts. J Neurosci Off J Soc Neurosci. 2002; 22:8891–8901.

McConnell HM, Radhakrishnan A. Condensed complexes of cholesterol and phospholipids. Biochim Biophys Acta. 2003; 1610:159–173. [PubMed: 12648771]

Middlemas DS, Raftery MA. Identification of subunits of acetylcholine receptor that interact with a cholesterol photoaffinity probe. Biochem (Mosc). 1987; 26:1219–1223.

Narayanaswami V, McNamee MG. Protein-lipid interactions and Torpedo californica nicotinic acetylcholine receptor function. 2. Membrane fluidity and ligand-mediated alteration in the accessibility of gamma subunit cysteine residues to cholesterol. Biochem (Mosc). 1993; 32:12420–12427.

O'Neill MJ, Murray TK, Lakics V, et al. The role of neuronal nicotinic acetylcholine receptors in acute and chronic neurodegeneration. Curr Drug Targets CNS Neurol Disord. 2002; 1:399–411. [PubMed: 12769612]

Ohlsson RI, Lane CD, Guengerich FP. Synthesis and insertion, both in vivo and in vitro, of rat-liver cytochrome P-450 and epoxide hydratase into *Xenopus laevis* membranes. Eur J Biochem FEBS. 1981; 115:367–373.

Oshikawa J, Toya Y, Fujita T, et al. Nicotinic acetylcholine receptor alpha 7 regulates cAMP signal within lipid rafts. Am J Physiol Cell Physiol. 2003; 285:C567–C574. [PubMed: 12748066]

Paterson D, Nordberg A. Neuronal nicotinic receptors in the human brain. Prog Neurobiol. 2000; 61:75–111. [PubMed: 10759066]

Pike LJ. Rafts defined: a report on the Keystone Symposium on Lipid Rafts and Cell Function. J Lipid Res. 2006; 47:1597–1598. [PubMed: 16645198]

Radhakrishnan A, McConnell HM. Condensed complexes of cholesterol and phospholipids. Biophys J. 1999; 77:1507–1517. [PubMed: 10465761]

Roher AE, Kuo YM, Kokjohn KM, et al. Amyloid and lipids in the pathology of Alzheimer disease. Amyloid Int J Exp Clin Investig Off J Int Soc Amyloidosis. 1999; 6:136–145.

Santiago J, Guzmán GR, Rojas LV, et al. Probing the effects of membrane cholesterol in the Torpedo californica acetylcholine receptor and the novel lipid-exposed mutation alpha C418W in Xenopus oocytes. J Biol Chem. 2001; 276:46523–46532. [PubMed: 11567020]

Schiebler W, Hucho F. Membranes rich in acetylcholine receptor: characterization and reconstitution to excitable membranes from exogenous lipids. Eur J Biochem FEBS. 1978; 85:55–63.

Sumikawa K, Houghton M, Emtage JS, et al. Active multi-subunit ACh receptor assembled by translation of heterologous mRNA in Xenopus oocytes. Nature. 1981; 292:862–864. [PubMed: 7196502]

Sunshine C, McNamee MG. Lipid modulation of nicotinic acetylcholine receptor function: the role of neutral and negatively charged lipids. Biochim Biophys Acta. 1992; 1108:240–246. [PubMed: 1379073]

Tamamizu S, Lee Y, Hung B, et al. Alteration in ion channel function of mouse nicotinic acetylcholine receptor by mutations in the M4 transmembrane domain. J Membr Biol. 1999; 170:157–164. [PubMed: 10430659]

Tamamizu S, Guzmán GR, Santiago J, et al. Functional effects of periodic tryptophan substitutions in the alpha M4 transmembrane domain of the Torpedo californica nicotinic acetylcholine receptor. Biochem (Mosc). 2000; 39:4666–4673.

Wood WG, Schroeder F, Igbavboa U, et al. Brain membrane cholesterol domains, aging and amyloid beta-peptides. Neurobiol Aging. 2002; 23:685–694. [PubMed: 12392774]

Yeagle PL. Cholesterol and the cell membrane. Biochim Biophys Acta. 1985; 822:267–287. [PubMed: 3904832]

Zhu D, Xiong WC, Mei L. Lipid rafts serve as a signaling platform for nicotinic acetylcholine receptor clustering. J Neurosci Off J Soc Neurosci. 2006; 26:4841–4851.

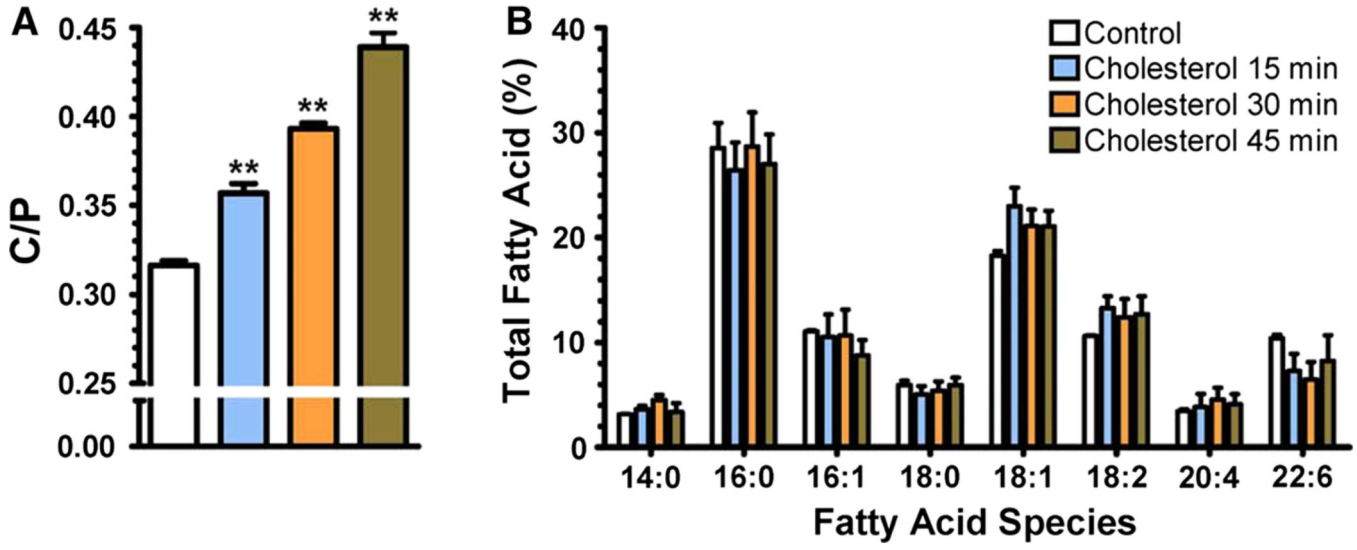

Fig. 1.

Increase in C/P in the plasmalemma of *Xenopus laevis* oocytes upon cholesterol enrichment. Cholesterol enrichment of *Xenopus laevis* oocytes was achieved by 15, 30, and 45 min incubations in cholesterol-rich DOPC liposomes. **a** Incubation of *Xenopus laevis* oocytes in cholesterol-rich DOPC liposomes resulted in significant increases in C/P (One-way ANOVA with Dunnett's post-test, $*P < 0.01$) when compared to control experiments (incubation in MOR2 buffer) without affecting the membrane fatty acid composition derived from phospholipid hydrolysis (**b**) (Two-way ANOVA with Bonferroni's post-test, $P > 0.05$). Experiments were performed in quadruplicate. Values are expressed as the percent of each fatty acid of the total free and esterified fatty acids in the phospholipids

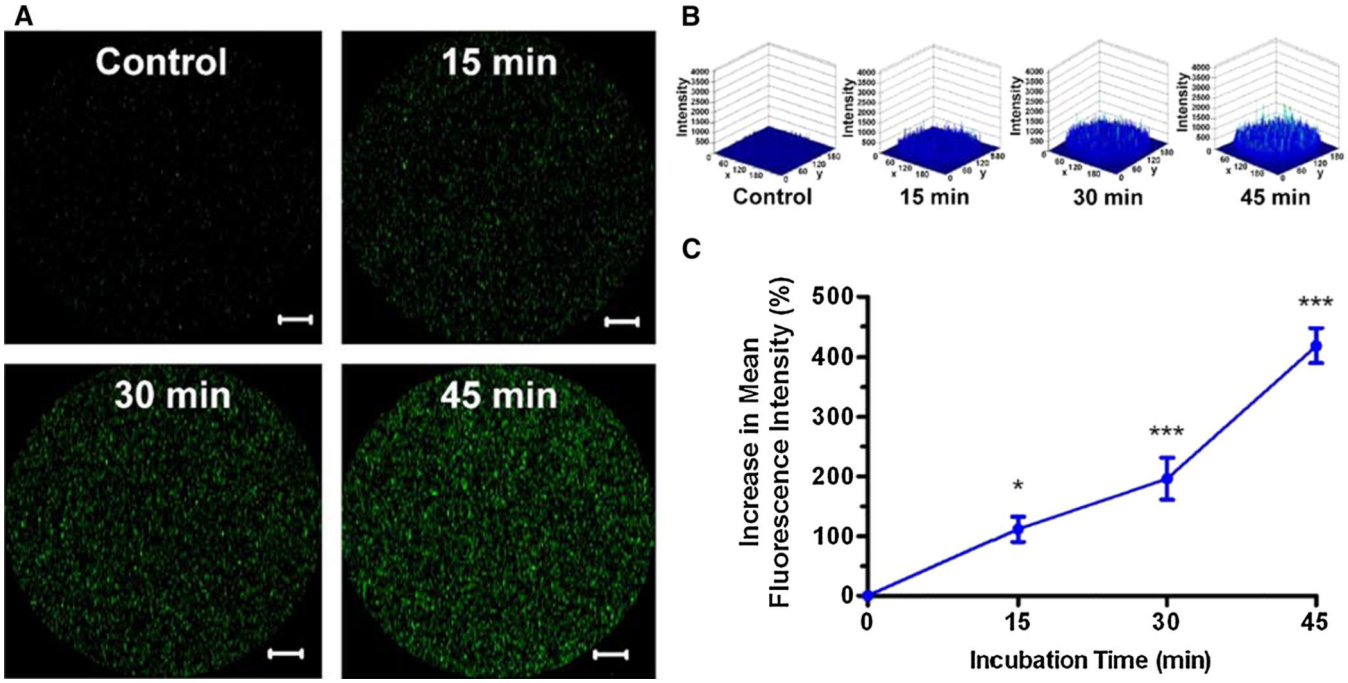

Fig. 2.

Incorporation of the fluorescent cholesterol analog into the plasmalemma of *Xenopus laevis* oocytes. The incorporation of cholesterol into the *Xenopus laevis* oocytes plasmalemma was monitored as function of time using DOPC liposomes enriched with the fluorescent cholesterol analog [(22-(N-(7-nitrobenz-2-oxa-1,3-diazol-4-yl)amino-22,23-bisnor-5-cholen-3-ol)]. The same incubation procedure employed to increase the oocytes membrane cholesterol concentration was used with the liposomes enriched with the fluorescent cholesterol analog and the incorporation was monitored through confocal microscopy. **a** Circular inserts (200 μm in diameter) of the oocytes plasmalemma display the incorporation of the fluorescent cholesterol as function of incubation time. Scale bar: 20 μm. The image displays a single optical slice acquired at a magnification of × 10. **b** Fluorescence intensity histograms highlight the increase in the fluorescence of the cholesterol analog in the oocytes plasma membrane as function of incubation time. The z-axis corresponds to the fluorescent intensity (a.u.), whereas the x- and y-axis correspond to spatial coordinates. **c** The cholesterol enrichment strategy was revalidated by the increase in fluorescence intensity of the fluorescent cholesterol analog in the oocytes plasmalemma upon incubation with cholesterol-rich DOPC liposomes (One-way ANOVA with Dunnett's post-test, 15 min $P < 0.05$; 30 min $P < 0.01$; 45 min $P < 0.01$; $n = 5$)

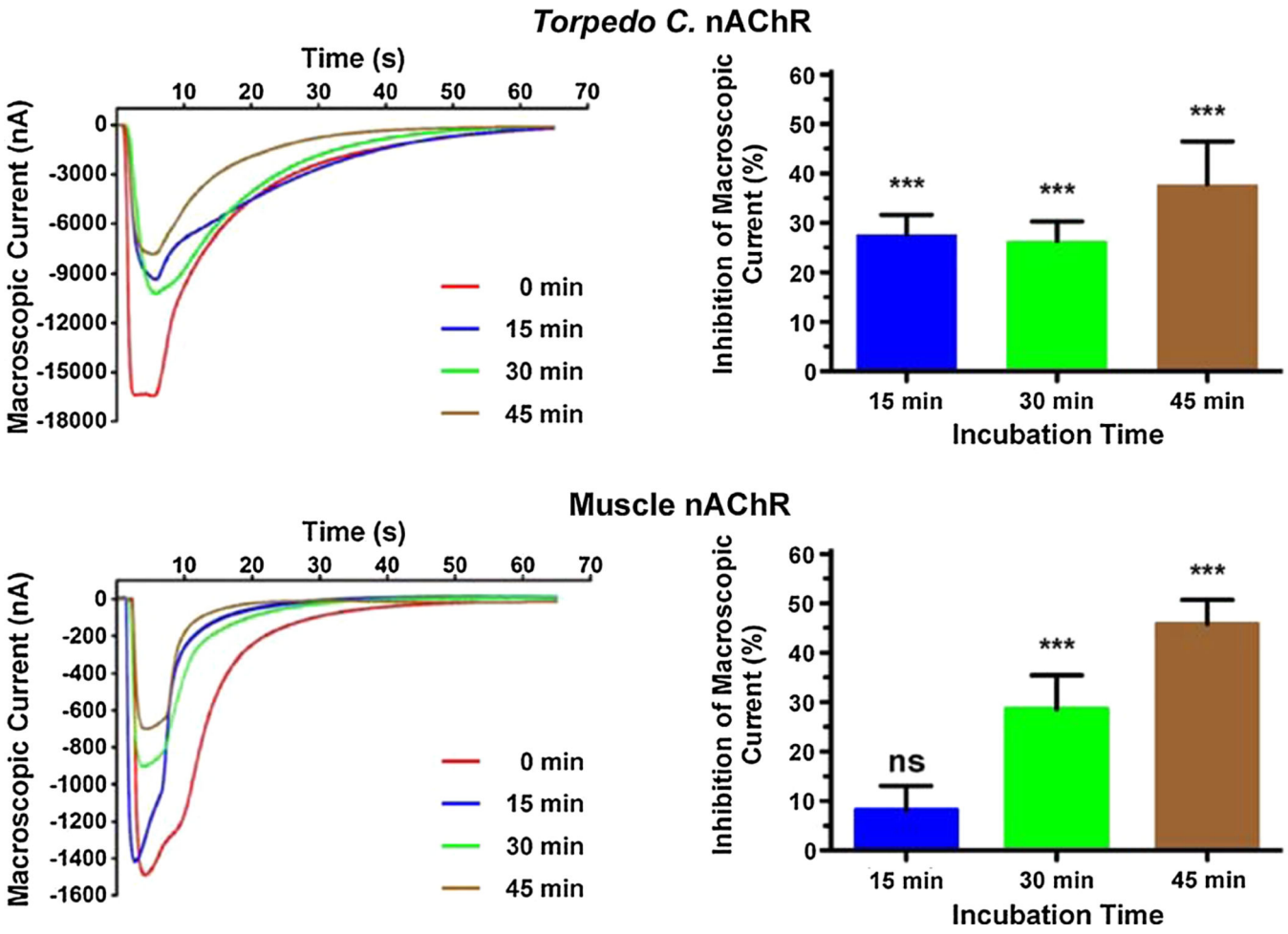

Fig. 3.

Increasing the C/P in the plasmalemma of *Xenopus laevis* oocytes results in a reduction in macroscopic currents in muscle-type and *Torpedo* nAChRs. Families of current traces elicited by 100 μM ACh demonstrate that the reduction in macroscopic currents upon cholesterol enrichment depends on the nAChR subtype expressed in the *Xenopus laevis* oocytes. The reductions in macroscopic current that result from 15, 30, and 45 min incubations in cholesterol-enriched DOPC liposomes are 28, 26, and 38 % in case of the *Torpedo* nAChR; and 8, 29, and 46 % in the muscle nAChR. The 15 min incubations resulted in statistically significant differences in macroscopic current reductions between the muscle and the *Torpedo* nAChR (*P* value = 0.0095, two-tailed, unpaired *t* test analysis, Table 1) (Color figure online)

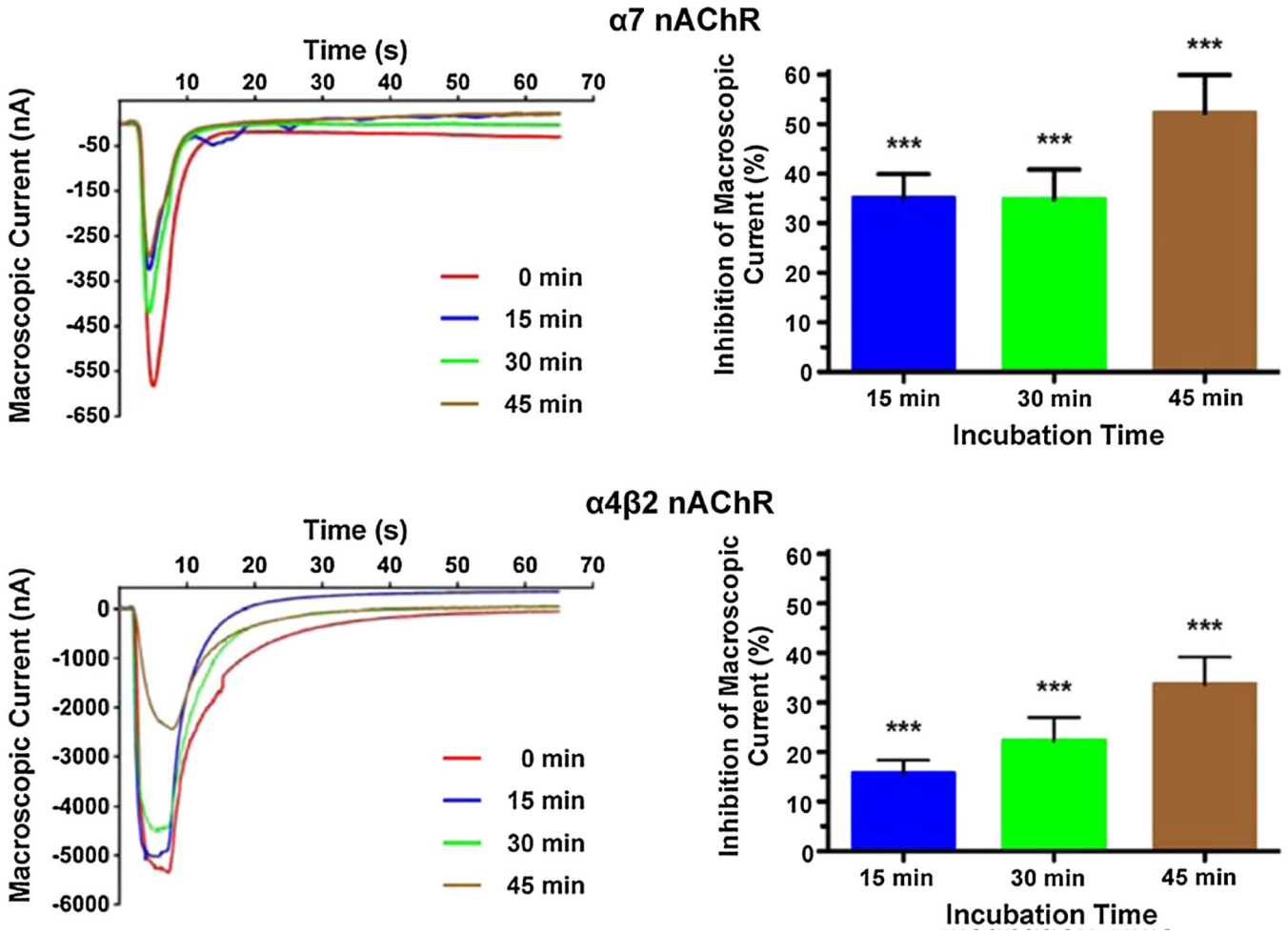

Fig. 4.

Increasing the C/P in the plasmalemma of *Xenopus laevis* oocytes results in a reduction in macroscopic currents in neuronal nAChRs α7 and α4β2. Current traces elicited by 100 μM ACh before and after membrane cholesterol enrichment demonstrate that the α7 nAChR functionality is more susceptible to increases in membrane cholesterol than the neuronal nAChR α4β2. The decrease in α7 nAChR macroscopic current upon 15, 30, and 45 min incubations in cholesterol-enriched DOPC liposomes was 35, 35, and 52 %, respectively, whereas the same incubations resulted in reductions in the α4β2 macroscopic currents of 16, 22, and 34 %, respectively. The 15 min incubations produced statistically different reductions in the α7 and α4β2 macroscopic currents (*P* value = 0.0006, two-tailed, unpaired *t* test analysis, Table 1) (Color figure online)

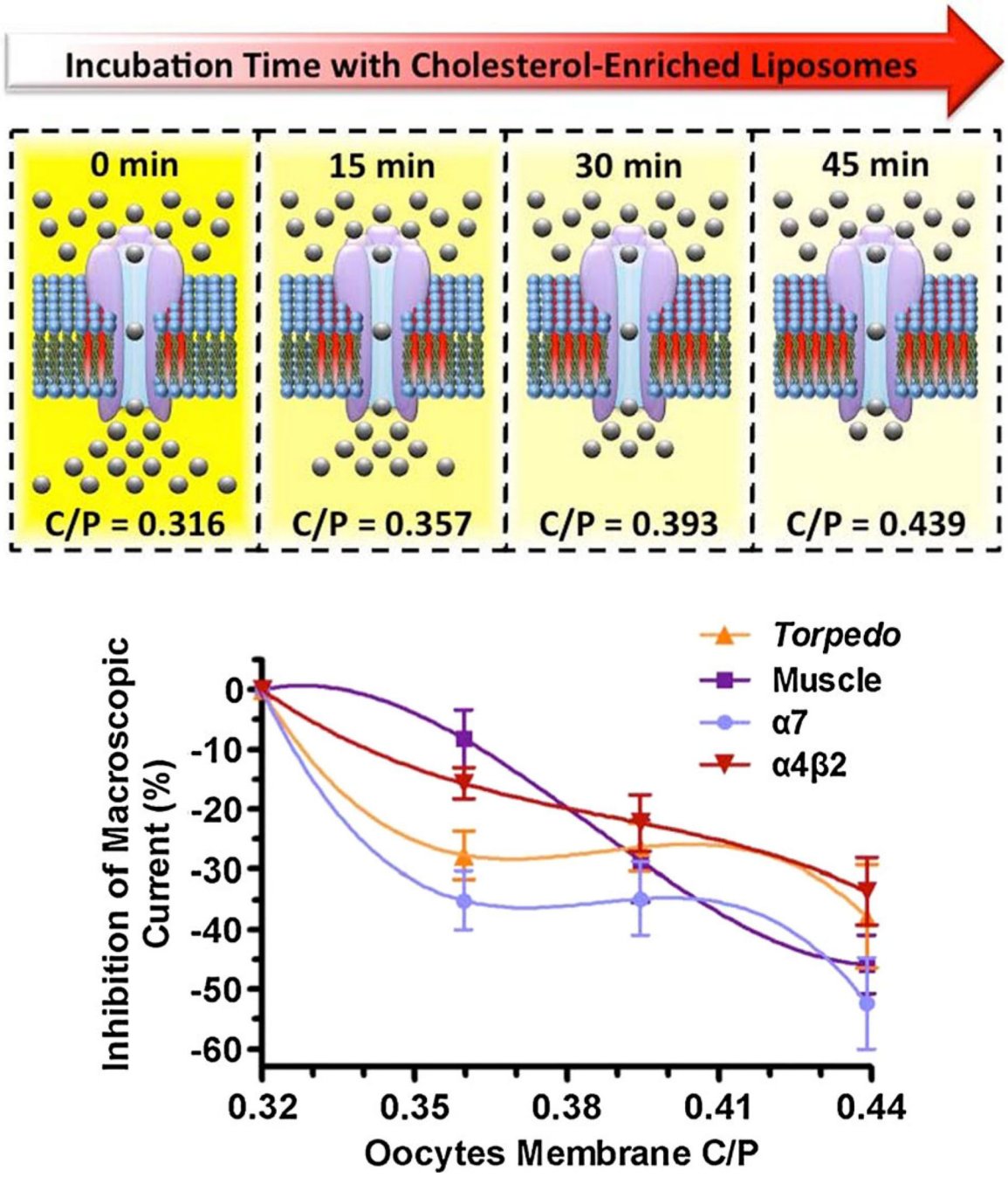

Fig. 5.

Profiles of the inhibition in function of the *Torpedo californica*, muscle, α7, and α4β2 nAChRs. By plotting the reduction in macroscopic current as function of the *Xenopus laevis* oocytes membrane C/P, the muscle nAChR inhibition profile reveals that the muscle type is the most tolerant receptor, among the four studied, to increases in membrane cholesterol concentrations

Table 1

Inhibition of nAChR subtypes by membrane cholesterol

Time (min)	Decrease in macroscopic current [% ± SEM (*n*)]			
	Torpedo	**Muscle**	**α7**	**α4β2**
15	28 ± 4 (19)	8 ± 5 (8)	35 ± 5 (21)	16 ± 3 (25)
30	26 ± 4 (14)	29 ± 7 (8)	35 ± 6 (15)	22 ± 5 (13)
45	38 ± 9 (10)	46 ± 5 (8)	52 ± 8 (11)	34 ± 6 (10)

Two-tailed, unpaired *t* test analysis. Statistically significant differences: *Torpedo* versus Muscle (15 min) $P = 0.0095$, *Torpedo* versus α4β2 (15 min) $P = 0.0126$, *Muscle* versus α7 (15 min) $P = 0.0035$, α7 versus α4β2 (15 min) $P = 0.0006$